



Contents lists available at ScienceDirect

Comparative Biochemistry and Physiology, Part A

journal homepage: www.elsevier.com/locate/cbpaCO₂ induced seawater acidification impacts sea urchin larval development II: Gene expression patterns in pluteus larvaeM. Stumpp^{a,*}, S. Dupont^b, M.C. Thorndyke^c, F. Melzner^a^a Biological Oceanography, Leibniz Institute of Marine Sciences (IFM-GEOMAR), 24105 Kiel, Germany^b Department of Marine Ecology, Sven Lovén Centre for Marine Sciences, Kristineberg, University of Gothenburg, Sweden^c The Royal Swedish Academy of Sciences, Sven Lovén Centre for Marine Sciences, Kristineberg, University of Gothenburg, Sweden

ARTICLE INFO

Article history:

Received 13 December 2010

Received in revised form 20 June 2011

Accepted 21 June 2011

Available online xxxx

Keywords:

Strongylocentrotus purpuratus

Echinoderm

Growth

RT-qPCR

Ocean acidification

ABSTRACT

Extensive use of fossil fuels is leading to increasing CO₂ concentrations in the atmosphere and causes changes in the carbonate chemistry of the oceans which represents a major sink for anthropogenic CO₂. As a result, the oceans' surface pH is expected to decrease by ca. 0.4 units by the year 2100, a major change with potentially negative consequences for some marine species. Because of their carbonate skeleton, sea urchins and their larval stages are regarded as likely to be one of the more sensitive taxa. In order to investigate sensitivity of pre-feeding (2 days post-fertilization) and feeding (4 and 7 days post-fertilization) pluteus larvae, we raised *Strongylocentrotus purpuratus* embryos in control (pH 8.1 and pCO₂ 41 Pa e.g. 399 µatm) and CO₂ acidified seawater with pH of 7.7 (pCO₂ 134 Pa e.g. 1318 µatm) and investigated growth, calcification and survival. At three time points (day 2, day 4 and day 7 post-fertilization), we measured the expression of 26 representative genes important for metabolism, calcification and ion regulation using RT-qPCR.

After one week of development, we observed a significant difference in growth. Maximum differences in size were detected at day 4 (ca. 10% reduction in body length). A comparison of gene expression patterns using PCA and ANOSIM clearly distinguished between the different age groups (two-way ANOSIM: Global R = 1) while acidification effects were less pronounced (Global R = 0.518). Significant differences in gene expression patterns (ANOSIM R = 0.938, SIMPER: 4.3% difference) were also detected at day 4 leading to the hypothesis that differences between CO₂ treatments could reflect patterns of expression seen in control experiments of a younger larva and thus a developmental artifact rather than a direct CO₂ effect. We found an up regulation of metabolic genes (between 10% and 20% in ATP-synthase, citrate synthase, pyruvate kinase and thiolase at day 4) and down regulation of calcification related genes (between 23% and 36% in msp130, SM30B, and SM50 at day 4). Ion regulation was mainly impacted by up regulation of Na⁺/K⁺-ATPase at day 4 (15%) and down regulation of NHE3 at day 4 (45%). We conclude that in studies in which a stressor induces an alteration in the speed of development, it is crucial to employ experimental designs with a high time resolution in order to correct for developmental artifacts. This helps prevent misinterpretation of stressor effects on organism physiology.

© 2011 Elsevier Inc. All rights reserved.

1. Introduction

Due to anthropogenic CO₂ emissions, atmospheric pCO₂ is expected to reach values of 70–100 Pa (ca. 700–1000 µatm) by the end of this century (Caldeira and Wickett, 2005; Cao and Caldeira, 2008). This increase in pCO₂ will alter ocean surface water carbonate chemistry, resulting in a reduction of ocean carbonate concentrations and a decrease in pH by up to ca. 0.4 units. It has been suggested that this progressive ocean acidification will negatively impact marine heterotrophic organisms by slowing calcification rates or even causing dissolution of carbonate shells

when saturation states of calcite (Ω_{calc}) or aragonite (Ω_{arag}) drop below unity (Orr et al., 2005; Hoegh-Guldberg et al., 2007). However, recent evidence indicates that elevated seawater pCO₂ impacts marine ectothermic organisms through multiple processes, such as disturbances in acid–base and ion homeostasis, metabolism, somatic growth and reproduction and thus not only impacts calcification. An altered energy partitioning between different physiological processes may be a key effect of seawater acidification on heterotrophic organisms (see Fabry, 2008; Pörtner and Farrell, 2008; Wood et al., 2008; Melzner et al., 2009; Dupont et al., 2010b for reviews).

In echinoderms, high mortalities and morphological abnormalities were observed in ophiuroid larvae exposed to a seawater pCO₂ of approximately 74 Pa (Dupont et al., 2008). Studies on other echinoderm species also reported growth delays (Kurihara and Shirayama, 2004; Kurihara, 2008; Clark et al., 2009; Brennand et al., 2010; O'Donnell et al.,

* Corresponding author at: Biological Oceanography, Leibniz-Institute of Marine Sciences (IFM-GEOMAR), Hohenberg Str. 2, 24105 Kiel, Germany.

E-mail address: mstumpp@ifm-geomar.de (M. Stumpp).

2010), and reduced fertilization success (Havenhand et al., 2008), but in other cases could increase developmental success (Dupont et al., 2010a) or had no measurable effect on development or fertilization (Carr et al., 2006; Byrne et al., 2009; Byrne et al., 2010a; Byrne et al., 2010b; Ericson et al., 2010) all at seawater $p\text{CO}_2$ values expected for the next century. These conflicting findings indicate high species specificity of seawater $p\text{CO}_2$ impacts on echinoderms (for review see Dupont et al., 2010b).

Because of the direct impacts of rising $p\text{CO}_2$ on the carbonate chemistry of seawater, calcification has been the primary target of previous investigations. Responses of various invertebrate taxa are diverse, ranging from reductions in calcification rates (Langdon and Atkinson, 2005; Shirayama and Thornton, 2005; Clark et al., 2009; Thomsen et al., 2010) to increases in calcification rates (Gutowska et al., 2008; Wood et al., 2008; Gutowska et al., 2010). In sea urchin larvae, reduced growth has been observed in several studies. Although calcification rates appeared to be normal in relation to size in *Paracentrotus lividus* larvae (Martin et al., 2011), it is unclear whether hypercapnia effects on growth are due to reductions in calcification performance or whether calcification is affected in a secondary fashion due to changes in somatic growth rate (Kurihara and Shirayama, 2004; Clark et al., 2009; Brennand et al., 2010; O'Donnell et al., 2010). The few studies examining calcification under high $p\text{CO}_2$ by means of gene expression analysis mainly observed a down regulation of genes connected with calcification in early sea urchin larval stages (Todgham and Hofmann, 2009; O'Donnell et al., 2010). In contrast, Martin et al. (2011) demonstrated that expression of calcification genes in *P. lividus* was increased in response to elevated $p\text{CO}_2$. In lecithotrophic *Crossaster papposus* larvae, no impact on calcification and a higher growth rate was detected (Dupont et al., 2010a), implying that not only calcification, but other processes such as feeding, metabolism or ion regulation are affected by elevated $p\text{CO}_2$. In fact, metabolism has been found to be up-regulated with increasing seawater $p\text{CO}_2$ in the blue mussel *Mytilus edulis* (Thomsen et al., 2010; Thomsen and Melzner, 2010) and the ophiuroid *Amphiura filiformis* (Wood et al., 2008), potentially reflecting elevated energetic costs for calcification and/or cellular homeostasis in some marine invertebrates that cannot control the carbonate system speciation in their extracellular fluids. In other invertebrate species, metabolic depression, elicited by uncompensated extracellular pH, has been suggested to occur (see Pörtner, 2008). In early sea urchin larvae, no metabolic rate measurements under acidified conditions have been performed so far, but a down-regulation of several metabolic genes (e.g. Succinyl-CoA synthetase, citrate synthase, pyruvate dehydrogenase, ATP synthase F1 complex) has been reported (Todgham and Hofmann, 2009; O'Donnell et al., 2010). This could support the metabolic depression hypothesis and explain reduced rates of growth.

In this paper, we used gene expression profiling in an explorative way to investigate, whether transcripts of genes with a crucial importance in metabolism, calcification and ion homeostasis are affected by near-future (year 2100) levels of seawater acidification in pre-feeding (day 2) and feeding (days 4 and 7) *Strongylocentrotus purpuratus* pluteus larvae. In a companion study (Stumpp et al., in press), we investigated the effects of $p\text{CO}_2$ on larval development success, morphology, feeding and metabolic rates. Larvae were raised at two seawater $p\text{CO}_2$ values: control (40 Pa, 399 μatm , pH 8.1) and elevated $p\text{CO}_2$ (134 Pa, 1318 μatm , pH 7.7).

2. Material and methods

2.1. Larval cultures

Adult *S. purpuratus* were collected on the Californian coast (Kerckhoff Marine Laboratory, California Institute of Technology, USA) and transferred to the Sven Lovén Center for Marine Sciences (Kristineberg, Sweden). They were fed *ad libitum* using *Ulva* spp. and

kept several weeks in flow-through systems with deep-water from the Gullmarsfjord before starting the experiment. Out-flow of the tanks was sterilized using UV-light to prevent introduction of the species into the fjord. Spawning was induced by injection of 2 mL 0.5 mM KCl into the coelomic cavity. Eggs of 3 females were collected in separate 1 L beakers and were washed and fertilized by adding dry sperm (20 μL) of one male. Fertilization was followed by monitoring the fertilization-induced elevation of the oocyte membrane under a stereomicroscope (fertilization rates >95%). Zygotes were allowed to divide once before they were pooled, concentrated in 25 mL and split into 50 L (1 replicate, polyethylene) and 5 L (3 replicates, Erlenmeyer flasks) culture vessels which were pre equilibrated with low (control) $p\text{CO}_2$ (ca. 40 Pa, 399 μatm) and high $p\text{CO}_2$ (ca. 134 Pa, 1318 μatm , pH 7.7; Table 1). Larvae in 50 L cultures grew slightly slower than in 5 L cultures. The initial larval concentration in each culture was 10 larvae mL^{-1} . Larval cultures were checked daily for health i.e. vitality of larvae and mortality. Culture vessels were kept in the dark and aerated with a stream of bubbles of pressurized air (ca. 100 bubbles of 4 mm diameter min^{-1}). Cultures were mixed by the slow convective current created by the motion of the bubbles in order to avoid disturbances of larvae by strong currents. Larvae of subsamples (two 10 mL samples per replicate) were enumerated daily for determination of culture densities. Larvae were collected in Eppendorf 1.5 mL tubes and fixed in 4% paraformaldehyde (PFA) in seawater pH 8.3 and stored at 4 °C for later morphometric measurements and determination of growth rates. Larvae started to feed when their digestive system was fully developed at ca. day 3. Larvae were fed with *Rhodomonas* spp. raised in B1 medium (Guillard and Ryther, 1962) at 20 °C under a 12:12 h light:dark cycle. Algal strains were provided by the Marine Algal Culture Centre at Gothenburg University (GUMACC). To prevent changes in food concentration, algae concentration and size were checked daily using a coulter counter (Elzone 5380, Micrometrics, Aachen, Germany) and then adjusted in the experimental bottles to the maximum concentration of 150 μg carbon L^{-1} (~3000 to 6000 cells mL^{-1} for diameters ranging between 7 and 9 μm). Seawater quality (e.g. presence of bacteria) was checked daily using the coulter counter and no water change was needed for the whole duration of the experiment. Samples for molecular biology were only taken from the 50 L culture replicates in order to sample sufficient amounts of larval tissue for the q RT PCR analysis.

2.2. pH regulation and carbonate chemistry measurements

Culture pH_{NBS} was kept stable (± 0.04 units) using Aqua Medic pH controllers (NBS scale, AquaMedic, Germany) that controlled valves for injection of pure CO_2 into the culture tanks once pH_{NBS} exceeded

Table 1

Experimental water chemistry. Salinity, temperature, total alkalinity (A_T) and pH were measured four times during the experimental period. C_T , calcite and aragonite saturation states and $p\text{CO}_2$ were calculated using CO2SYS software (Lewis and Wallace, 1998).

	Control pH 8.2	Low pH 7.7
<i>Measured</i>		
Salinity	32.0 \pm 0.7	32.0 \pm 0.7
Temperature (°C)	16.0 \pm 0.8	16.0 \pm 0.8
A_T ($\mu\text{mol kg}^{-1}$)	2243 \pm 40	2233 \pm 17
pH_{NBS}	8.17 \pm 0.04	7.70 \pm 0.04
<i>Calculated</i>		
C_T ($\mu\text{mol kg}^{-1}$)	2035 \pm 38	2196 \pm 17
Ω_{Ca}	3.64 \pm 0.06	1.38 \pm 0.01
Ω_{Ar}	2.33 \pm 0.04	0.88 \pm 0.01
$p\text{CO}_2$ (Pa)	40.4 \pm 0.7	133.5 \pm 1.0
$p\text{CO}_2$ (μatm)	399 \pm 7	1318 \pm 10

the target value by more than 0.03 units. The Aqua Medic pH electrodes were cross-calibrated regularly with a Metrohm (827 pH lab) pH_{NBS} meter in order to ensure comparability between replicates. Total alkalinity (A_T) measurements were conducted four times during the experiment as described by Sarazin et al. (1999) with an accuracy of $10 \mu\text{mol kg}^{-1}$ seawater. Total dissolved inorganic carbon (C_T), $p\text{CO}_2$ and calcium carbonate saturation states for calcite (Ω_{calc}) were calculated from A_T and pH_{NBS} using CO2SYS software (Lewis and Wallace, 1998, Table 1). Salinity and temperature were measured four times (Table 1).

2.3. Sampling

Sampling was conducted at days 2, 4 and 7 post-fertilization in both treatments. At each time point, 20 samples of 3000 to 4000 larvae were taken from each culture, briefly concentrated in Eppendorf 1.5 mL tubes by means of hand centrifugation for 10 s at approximately 156 g. Excess water was discarded except for approximately 80 μL containing the larvae. Samples were then shock-frozen in liquid nitrogen. The whole sampling process took approximately 45 s per sample. Samples were stored at -80°C for ca. 6 months until further processing.

2.4. qRT-PCR

Total RNA was extracted from 3000 to 4000 larvae per sample using the Qiagen RNeasy Mini kit (Qiagen, Hilden, Germany) following the instruction manual. qRT-PCR analysis was carried out using the two step real-time RT-PCR method described by Vandenbroucke et al. (2001). Prior to cDNA synthesis, 3 to 10 μg total RNA (Nanodrop Bioanalyzer) was treated with DNase (Ambion by Applied Biosystems, Darmstadt, Germany) to digest genomic DNA remains. For cDNA synthesis, 0.4 μg total RNA (Nanodrop bioanalyzer) was transcribed using the Applied Biosystems High Capacity cDNA Reverse Transcriptase kit (Applied Biosystems, Darmstadt, Germany).

Primer Express Software (version 2.0 by Applied Biosystems) and sequences from the *S. purpuratus* genome were used to design primer pairs for 27 genes (Table 2). Efficiency was evaluated by applying the dilution standard curve method (dilution steps: 1:20; 1:100; 1:500; 1:2500 and 1:12,500). Primer concentrations were 300 nM. The *Taq* DNA polymerase was activated for 10 min at 95°C . Each PCR was run for 40 cycles at 95°C for 15 s and 62°C for 1 min. Subsequent to each PCR, a melting curve analysis was conducted. Each PCR of a total volume of 20 μL consisted of 2 μL template (cDNA dilution of 1:20), 3 μL of each primer (forward, reverse), 2 μL DNase free H_2O and 10 μL SYBR Green master mix (Platinum SYBR Green qPCR SuperMix-UDG with ROX, Invitrogen, Karlsruhe, Germany). Controls were conducted without template (no template control) and with RNA post DNase digestion to test for genomic DNA contamination within the cDNA. No significant DNA contamination was observed. Using LinRegPCR software version 7.4 (Ramakers et al., 2003) the PCR efficiency of each PCR reaction was determined. Efficiencies were always >1.9 . Real time qPCR measurements were conducted on a StepOnePlus real time cyler (Applied Biosystems, Darmstadt, Germany).

2.5. Gene normalization and statistical analysis

To identify suitable reference genes, NormFinder (Andersen et al., 2004) software was used (version 19). NormFinder uses an algorithm to estimate the overall expression variation as well as the variation between samples of subgroups of the sample set and is aiming at identifying a candidate gene with lowest intra-group variability and at the same time an inter-group variation as close to 0 as possible (Andersen et al., 2004). As data input for NormFinder (<http://www.mdl.dk/publicationsnormfinder.htm>), we used Ct values of all 27 gene transcripts from all treatment groups which were transformed into

quantities (Q) using the appropriate PCR efficiencies as determined using LinReg PCR using formula (1):

$$Q = E^{(-Ct)} \quad (1)$$

with E being the reaction specific efficiency (maximum efficiency of 100% would be 2, i.e. a doubling in the amount of PCR product per reaction cycle) and Ct being the Ct value as determined using StepOnePlus real time cyler software (adapted from Livak and Schmittgen, 2001). NormFinder suggested sodium bicarbonate cotransporter (NBC3, NCBI accession no: NM_001079551) to be the most stably expressed gene with an inter- and intra-group specific variation closest to zero (NormFinder stability values for NBC 0.001 to 0.006). NBC3 was thus used as reference gene for normalization.

For statistical reasons logarithmic Ct-values were converted into quantities (Q) using formula (1). Values were then normalized using the reference gene NBC3. A Bray–Curtis similarity analysis was conducted with square root transformed expression values (normalized quantities). From this similarity matrix, an analysis of similarity (one-way ANOSIM, two-way crossed ANOSIM using time and $p\text{CO}_2$ as factors), a Cluster analysis (principal component analysis, PCA) and a similarity of percentage analysis (SIMPER) analysis were carried out. The principal component analysis (PCA) with a cluster plot was used to determine the contribution of single genes to the observed sample pattern and test if genes from one pathway correlate in their expression behavior (e.g. ion regulation, calcification and metabolism). One-way and two-way crossed ANOSIM was chosen as non-parametric statistical method to analyze the significance in grouping elicited by the group specific gene expression patterns and determine the impact of $p\text{CO}_2$ and time on the observed pattern. A SIMPER analysis was then used to quantitatively determine the contribution of single genes to the observed similarity or dissimilarity between gene expression patterns of groups. All multivariate statistics including PCA were conducted using Primer 6 software (version 6.1.9; Primer-E Ltd.). For the evaluation of mortality and growth, t-tests and an analysis of covariance (ANCOVA) with log transformed data, respectively, were applied.

3. Results

Culture vessels had a salinity of 32 ± 0.7 and a temperature of $16 \pm 0.8^\circ\text{C}$. pH_{NBS} was maintained at 8.17 ± 0.04 in control and 7.70 ± 0.04 in low pH treatments. Total alkalinity (A_T) reached values of $2243 \pm 40 \mu\text{mol kg}^{-1}$ in control and $2233 \pm 17 \mu\text{mol kg}^{-1}$ in the low pH treatment. From these values a C_T of 2035 ± 38 and $2196 \pm 17 \mu\text{mol kg}^{-1}$ and a $p\text{CO}_2$ of 40 Pa and 134 Pa (i.e. 399 μatm , 1318 μatm) in control and low pH vessels respectively, were calculated. The experimental seawater was super saturated with calcite and aragonite under control conditions (3.64 ± 0.06 and 2.33 ± 0.04 , respectively). Under low pH conditions, the experimental water was still super saturated with calcite (1.38 ± 0.01), while Ω_{arag} was <1 (0.88 ± 0.01).

As an indicator of the health of cultures and larvae, their relative density during the experimental period was determined daily while length parameters of larvae (total length, arm length, $n=20$) were measured at days 2, 4 and 7. After 7 experimental days, a decrease in relative larval density was detected in the cultures, with values of 0.94 for the control treatment and 0.86 for the acidified condition (Fig. 1A). The difference of 0.08 between treatments was not statistically significant (ANOVA, day 7, $p=0.77$).

Growth (total length) of larvae followed a logarithmic curve for control as well as for the low pH treatment group (Fig. 1B). Growth (total length) of larvae was significantly affected by acidification of the water (growth rate comparison on body length vs. log transformed time, ANCOVA, $p<0.001$). The smallest size difference (5.9%) was observed at culture day 7, a maximum size difference (10%) was

Table 2
Primer data for RT-qPCR for 27 observed genes including primer description, primer sequence (forward F, reverse R), amplicon length and PCR efficiency for the respective PCR reaction (determined by LinRegPCR).

ID	Primer name/ abbreviation	Gene/protein description	Primer sequence	Amplicon length (bp)	Primer efficiency	NCBI accession no.
1	AE3a F AE3a R	Chloride/bicarbonate exchanger, anion exchanger 3-like protein, SLC4A3	AAGATCCCGCCGACTCT ATGTACGGTGCCTCAAGGTACTC	71	1,96	XM_788556
2	AE3b F AE3b R	Anion exchanger 3, SLC4A3	AGGTGCCTCTAGCCGTCTCT TCTCTACCATTGGATACCATTTGAGT	78	1,95	XM_001195823
3	ATP-S F ATP-S R	ATP-synthase β -subunit	TTCTTGCCCAACCCITCCA TCTGCCATCGAGACGAGCTT	71	1,97	NM_001123502
4	CA15 F CA15 R	Carbonic anhydrase 15 α -subfamily (CA15)	CTTGACATGTTCCGTGAGCTTTA CGATGTGGAGCATCTCCAGTT	73	1,95	XM_001177813 SPU_012518
5	CA10 F CA10 R	Carbonic anhydrase related protein (CARP 10)	CATATCAGGAGGCCATTGAG TATTCTCCCGCGAAGTG	71	1,97	XM_001182003.1
6	CS F CS R	Citrate synthase	CTTCCCACGTGCGAGAT AGCGGCACTGAATTGAGACA	71	1,96	XR_026166
7	EN F EN R	(Similar to) Echinonectin	AGTCAGGTGGTAACGGTTGGA GTCGCCGAGATCCACCATAA	71	1,94	XM_001184352
8	FACT F FACT R	Facilitates chromatin transcription (FACT) complex subunit SPT16	CCTGCCACCACCGTCTA GAGCGGGATCGTTTCTCTT	71	1,96	XM_001203176
9	gp96 F gp96 R	Heat shock protein gp96	CTTTTAGCCATCGTAGGTGTTCTG CAACAATTGCCCTCTCCCTCATC	79	1,97	NM_214643
10	HSP70 F HSP70 R	Heat shock protein 70 kDa	GCCATGTAAGAAGGCCATTGAG CCACCGACGAGCAGAACCT	72	1,97	XM_776184
11	IR F IR R	Mannose-6-phosphate/insulin-like growth factor II receptor	TGACACCCTGCAGCTTACGAT TGCAAACGCTTCCCCTGTA	71	1,97	XR_025889
12	lys-H ⁺ -ATPase F lys-H ⁺ -ATPase R	Lysoosomal H ⁺ -ATPase	CAACGACTGACCCAGAGTATCTA CCACTTCTGGTGGCAGCTGA	73	1,93	XR_026057
13	MMP F MMP R	Matrix-metalloproteinase 14	TCCCAAGGCCGACATCAT CAGGGCCATCGAAGCATAA	71	1,97	XM_001175853 SPU_013670
14	msp 130 F msp 130 R	Mesenchyme-specific cell surface glycoprotein msp 130	CTTCAACGGAGCCGCATT TCGATCGCGAGTCTTAGTCA	71	1,96	XM_001179349
15	NKA F NKA R	Sodium/potassium ATPase alpha subunit (NKA, Na ⁺ /K ⁺ -ATPase)	GGTGGTCAATTTGACAAAGTCTTCA TCAGATCGGTTGAGAGACAAA	74	1,95	XM_001202868
16	NBC3 F NBC3 R	Sodium/bicarbonate cotransporter 3, SLC4A7 (NBC3)	CCAACATCCAGAACAGCCAAA CTTGCCAGGTACCAGAGT	71	1,96	NM_001079551
17	NHE3 F NHE3 R	Sodium/hydrogen exchanger 3, SLC9A3 (NHE3, Na ⁺ /H ⁺ exchanger)	CATCCCGGTGTATCG TGCGTGATGACTTTAGAACAACA	61	1,96	XM_001178217
18	PK F PK R	(Similar to) Pyruvate kinase type M2	CGCCACAGCCAACACATTC TGCTGGAGGGGATTCAAT	62	1,97	XR_025967
19	SERCA F SERCA R	Sarco/endoplasmic reticulum calcium transporting ATPase (SERCA)	ACCTCCCAAGAGCAAGA CATCACCCGTCATAGCTGTGA	71	1,95	NM_001037630
20	SM30B F SM30B R	Spicule matrix protein 30 B	TCGACAGTGGTGTCTTCTTGA AAGGCCGTTCTCGTTGTGA	71	1,94	XM_001175556 SPU_000826
21	SM30E F SM30E R	Spicule matrix protein 30 E	GGAACCTTAATGCCAACCTACTC TGGATTATGGGTCCAGTGCAA	71	1,97	XM_001177597 SPU_004867
22	SM50 F SM50 R	Spicule matrix protein 50	GGCTCCGAATCTGTGAAA CTGAAGCCAGAGCACCCATT	71	1,97	NM_214610 SPU_018811
23	β -Actin F β -Actin R	β -Actin	CGTCGTTTACATCATTCGGACAT GACCCGTTGTCGATGACGAT	71	1,96	XM_001176939.1
24	TBP F TBP R	TATA-box binding protein (TBP)	AGTTCACAGCAGAGTCAGTCCCTA CTACCCACCGAACCAACGA	71	1,94	NM_214621
25	T F T R	Thiolase: hydroxyacyl-coenzyme A dehydrogenase	AAGCCAGCACTTCTTTGGTT GGGACGTCACGACTACTTC	71	1,97	XM_001192117
26	V-H ⁺ -ATPase F V-H ⁺ -ATPase R	Vacuolar (v-type) H ⁺ -ATPase B subunit, transcript variant 2 (V-type H ⁺ -ATPase)	GTCCGTGCTCGTGAAGAAG TGGTTGCCAAATCAGTGTACATG	71	1,96	XM_001176838
27	VSOP F VSOP R	Voltage gated proton channel (VSOP)	ATCGTCGAGCTGTGCTGACTT TCCGTCTCTGTGCAATTGCA	71	1,96	NM_001126307

observed at culture day 4 (Fig. 1). Proportions of larvae measured by the additional morphometric parameters that included post-oral rod and postero-lateral rod, revealed that larvae reared under elevated seawater $p\text{CO}_2$ were not only smaller, but exactly matched the morphometric parameters characteristic for earlier larval age (Stumpp et al., in press). Thus, we used body length to normalize the detected morphological developmental delay caused by ocean acidification in order to estimate, whether changes in gene expressions are direct effects of elevated seawater $p\text{CO}_2$ or indirect effects caused by the growth delay itself.

Gene expression patterns for candidate genes involved in ion transport (8 genes), calcification (8 genes), metabolism (5 genes), the cellular stress response (2 genes) and reference (4 genes) were assessed in *S. purpuratus* larvae cultured under control (pH_{NBS} : 8.2, $p\text{CO}_2$: 40 Pa,

399 μatm) and acidified (pH_{NBS} : 7.7, $p\text{CO}_2$: 134 Pa, 1318 μatm) conditions, sampled at 3 time points (2, 4, and 7 days post-fertilization). Highest gene transcript levels within the 26 genes studied were those of ATP-Synthase, Na⁺/K⁺-ATPase and SM30B, with values of 25.9, 17.1 and 15.6 relative to NBC, respectively (Table 3). Transcript levels of almost all genes changed strongly during the first seven days of development (except NHE3). Developmental time had a much stronger influence on sea urchin gene expression patterns than CO₂ enrichment of the culture medium. Using principal component analysis (PCA, Fig. 3) and an analysis of similarity (ANOSIM: one-way, two-way crossed, Table 4) including the test for contribution of the genes to the similarity pattern (SIMPER, e.g. similarity percentage, Table 5), we analyzed changes in gene expression patterns overall to determine stage effects and stage independent acidification effects. Overall, the gene expression

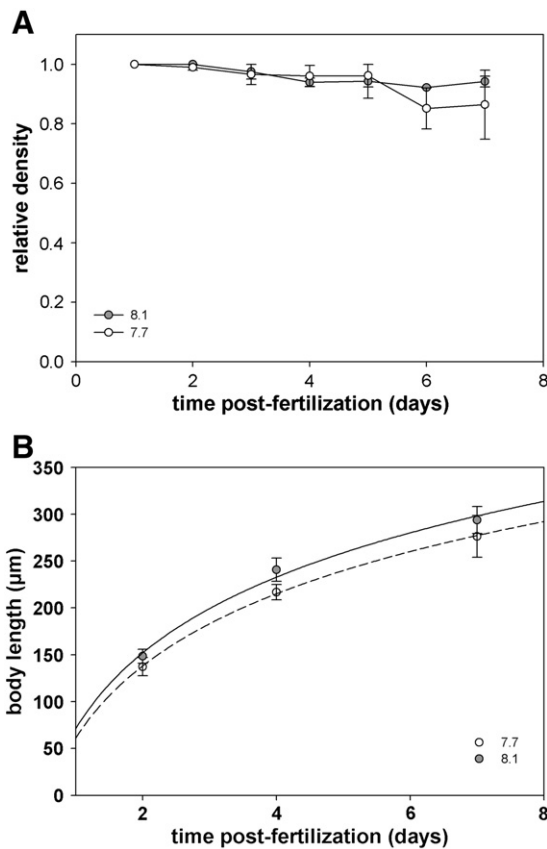


Fig. 1. Performance data for *Strongylocentrotus purpuratus* larval cultures. A: relative density (mean ± SD) of larvae in control (8.1) and acidified (7.7) treatments during the experimental period (n = 3). B: larval growth rate as body length (mean ± SD; n = 20) under control (8.1) and acidified (7.7) conditions (for more morphological details of larvae see also Stumpp et al., in press).

Table 3

Gene expression data for control and low pH (e.g. pH 7.7) treatments at three time points (days 2, 4 and 7 post-fertilization): Ct values were transformed into quantities incorporating PCR efficiencies and normalized against NBC3 as suggested by 'NormFinder'. The change in gene expression (% change) was calculated from control to low pH.

Genes	Culture day 2			Culture day 4			Culture day 7		
	Control	Low pH	% change	Control	Low pH	% change	Control	Low pH	% change
Ion transport									
AE3a	0.83 ± 0.09	0.85 ± 0.07	3.1	0.37 ± 0.02	0.33 ± 0.03	-11.3	0.34 ± 0.03	0.28 ± 0.02	-18.5
AE3b	0.11 ± 0.01	0.11 ± 0.01	-3.8	0.07 ± 0.00	0.07 ± 0.00	1.2	0.11 ± 0.01	0.10 ± 0.01	-1.7
Lys-H ⁺ -ATPase	1.29 ± 0.13	1.27 ± 0.08	-1.1	1.28 ± 0.14	1.34 ± 0.10	4.7	1.52 ± 0.09	1.44 ± 0.12	-5.3
NHE3	0.34 ± 0.02	0.38 ± 0.03	9.2	0.32 ± 0.02	0.17 ± 0.02	-45.4	0.33 ± 0.02	0.28 ± 0.02	-15.7
VSOP	0.37 ± 0.04	0.37 ± 0.03	-0.7	0.13 ± 0.01	0.13 ± 0.01	-2.4	0.31 ± 0.02	0.36 ± 0.03	16.4
V-H ⁺ -ATPase	2.53 ± 0.28	2.42 ± 0.20	-4.5	2.65 ± 0.23	2.63 ± 0.09	-0.6	3.57 ± 0.22	3.23 ± 0.19	-9.5
SERCA	4.19 ± 0.29	4.31 ± 0.14	2.7	5.10 ± 0.28	5.44 ± 0.28	6.8	3.71 ± 0.16	2.91 ± 0.16	-21.6
NKA	14.83 ± 0.98	14.78 ± 0.86	-0.3	17.08 ± 0.91	19.74 ± 1.57	15.6	12.68 ± 0.75	12.14 ± 1.06	-4.3
Calcification									
CA15	1.40 ± 0.12	1.23 ± 0.08	-11.7	0.73 ± 0.08	0.73 ± 0.06	0.2	0.50 ± 0.04	0.54 ± 0.03	7.0
CA10	0.24 ± 0.02	0.19 ± 0.02	-18.8	0.46 ± 0.04	0.44 ± 0.03	-5.4	0.56 ± 0.02	0.52 ± 0.04	-8.1
EN	0.32 ± 0.04	0.28 ± 0.02	-11.6	0.57 ± 0.05	0.46 ± 0.04	-18.8	1.26 ± 0.10	1.24 ± 0.12	-1.7
MMP	0.71 ± 0.06	0.67 ± 0.05	-5.5	0.22 ± 0.02	0.17 ± 0.01	-24.5	0.13 ± 0.01	0.12 ± 0.01	-7.5
msp130	6.40 ± 0.31	6.16 ± 0.45	-3.7	2.01 ± 0.11	1.28 ± 0.08	-36.3	0.76 ± 0.08	0.71 ± 0.05	-7.1
SM30B	15.61 ± 2.08	13.74 ± 1.46	-11.9	9.53 ± 0.63	6.79 ± 0.80	-28.8	4.05 ± 0.23	4.23 ± 0.33	4.5
SM30E	0.10 ± 0.01	0.12 ± 0.02	16.6	0.12 ± 0.01	0.11 ± 0.01	-8.9	0.06 ± 0.01	0.08 ± 0.02	41.7
SM50	5.10 ± 0.36	4.92 ± 0.46	-3.5	2.55 ± 0.12	1.96 ± 0.13	-23.2	1.27 ± 0.07	1.18 ± 0.14	-6.6
Metabolism									
ATP-synthase	11.71 ± 0.91	11.25 ± 0.96	-3.9	21.99 ± 2.10	25.84 ± 1.92	17.5	25.92 ± 1.36	28.01 ± 2.90	8.1
CS	2.75 ± 0.24	2.61 ± 0.30	-4.9	4.11 ± 0.44	4.62 ± 0.31	12.4	4.56 ± 0.25	4.91 ± 0.47	7.5
PK	0.55 ± 0.03	0.53 ± 0.05	-2.8	1.18 ± 0.12	1.29 ± 0.09	9.5	0.73 ± 0.05	0.86 ± 0.09	18.8
T	2.33 ± 0.16	2.16 ± 0.19	-7.0	3.28 ± 0.30	3.92 ± 0.24	19.7	1.48 ± 0.11	1.48 ± 0.16	-0.4
IR	0.46 ± 0.06	0.41 ± 0.03	-11.5	0.43 ± 0.04	0.44 ± 0.02	0.9	0.85 ± 0.02	0.93 ± 0.06	9.7
Heat shock proteins									
gp96	6.16 ± 0.79	5.61 ± 0.44	-9.0	6.46 ± 0.42	6.86 ± 0.21	6.2	4.32 ± 0.32	3.89 ± 0.36	-9.9
HSP70	3.54 ± 0.29	3.46 ± 0.28	-2.2	10.20 ± 0.51	12.08 ± 0.67	18.5	3.84 ± 0.28	3.40 ± 0.29	-11.6
Reference genes									
FACT	0.53 ± 0.02	0.51 ± 0.03	-2.6	0.65 ± 0.05	0.74 ± 0.05	13.7	0.43 ± 0.03	0.41 ± 0.03	-4.5
β-actin	1.59 ± 0.14	1.45 ± 0.11	-8.9	1.07 ± 0.13	1.26 ± 0.06	17.4	1.42 ± 0.08	1.67 ± 0.14	17.3
TBP	0.15 ± 0.01	0.14 ± 0.01	-5.4	0.23 ± 0.02	0.24 ± 0.01	2.9	0.14 ± 0.01	0.15 ± 0.01	4.3

Table 4

Summary of ANOSIM analyses based on the Bray–Curtis similarity matrix (square root transformed gene quantities). In the one-way ANOSIM, the six groups were independently analyzed, while factor influence (culture time and pH treatment) was analyzed with help of two-way crossed ANOSIM. R-values higher than 0.6 indicate significant differences, R-values of 0.4 to 0.6 display significant differences with some correlation between treatments, and values lower than 0.4 indicates no significant separation between groups.

ANOSIM (one-way)					
	Day 2 control	Day 2 low pH	Day 4 control	Day 4 low pH	Day 7 control
Day 2 low pH	0.084				
Day 4 control	1	1			
Day 4 low pH	1	1	0.938		
Day 7 control	1	1	1	1	
Day 7 low pH	1	1	1	1	0.533
Global R	0.91				
ANOSIM (two-way crossed)					
Global R _(culture time)					1
Global R _(pH treatment)					0.518

patterns (of the studied genes) of all 6 groups (day 2: pH 8.1 and 7.7; day 4: pH 8.1 and 7.7; day 7: pH 8.1 and 7.7) were characterized by a similarity of greater than 85% (based on a Bray–Curtis matrix).

A principal component analysis was applied to analyze the contribution of single genes to the observed patterns (Fig. 3). Principal components (PC) 1 and 2 explain over 96% of the observed variation with PC1 being the more important component, responsible for 70.1% of the measured variation.

Calcification genes, such as SM30, SM50, msp130, CA15, and MMP all contributed negatively to principal component 1 (PC1). ATP-synthase, citrate synthase and CA10 contributed positively to PC1. PC2 is not as obviously organized, with mainly Na⁺/K⁺-ATPase and HSP70 contributing negatively.

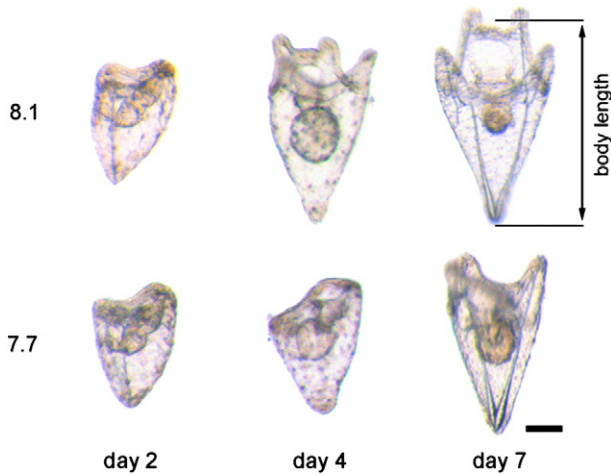


Fig. 2. Representative pictures of *Strongylocentrotus purpuratus* larvae at days 2, 4 and 7 post-fertilization at two pCO₂ treatments: control (pH 8.1) and acidified condition (pH 7.7). Scale bar (100 μm) is valid for all pictures. Measurement of body length used for growth rate is indicated for 7 day old pluteus larvae under control conditions (pH 8.1).

Testing all groups independently (6 groups: two CO₂ treatments, three time points) using one-way analysis of similarity (ANOSIM) (Table 4) revealed distinct differences in the gene expression patterns between culture days with R values of 1. Results for the CO₂ treatments were more variable showing no differences between treatment groups at culture day 2 with an R value of 0.084, while at culture day 4, an R value of 0.983 indicated significant differences between CO₂ treatments. This can also be seen in the distinct separation of the treatment groups at culture day 4 in the sample plot overlaying the PCA (Fig. 2). At culture day 7, the observed differences are still pronounced with an R value of 0.533, but not as clear as at culture day 4 which is also obvious in the sample plot

Table 5

Summary of SIMPER analysis based on the Bray-Curtis similarity matrix (square root transformed transcript abundance) showing only results for dissimilarity between treatment groups at the three sample time points 2, 4 and 7 days post-fertilization. Only genes with a dissimilarity contribution >5% are shown.

	Gene	pH 8.1 average abundance	pH 7.7 average abundance	Average dissimilarity	Contribution (%)
Day 2 (post-fert) average dissimilarity 2.60%	SM30B	3.94	3.7	0.4	15.26
	ATP-synthase	3.42	3.35	0.22	8.46
	gp96	2.48	2.37	0.2	7.53
	NKA	3.85	3.84	0.17	6.66
	SM50	2.26	2.22	0.14	5.31
	CS	1.66	1.61	0.13	5.08
Day 4 (post-fert) average dissimilarity 4.30%	SM30B	3.09	2.6	0.63	14.62
	ATP-synthase	4.68	5.08	0.55	12.74
	NKA	4.13	4.44	0.4	9.36
	msp130	1.42	1.13	0.37	8.63
	HSP70	3.19	3.48	0.37	8.53
	SM50	1.6	1.4	0.26	5.96
Day 7 (post-fert) average dissimilarity 3.06%	T	1.81	1.98	0.22	5.19
	ATP-synthase	5.09	5.29	0.45	14.81
	SERCA	1.93	1.7	0.32	10.58
	NKA	3.56	3.48	0.22	7.21
	HSP70	1.96	1.84	0.19	6.21
	gp96	2.08	1.97	0.19	6.19
	CS	2.14	2.21	0.17	5.5

(Fig. 2). These results were confirmed in a two-way crossed ANOSIM, which reveals that the impact of culture time on gene expression pattern and thus dissimilarity of groups is much more pronounced (R = 1) than the impact of CO₂ treatment (R = 0.518). Nevertheless, the differences between CO₂ treatments are still larger than would be expected by chance. Although CO₂ treatments/time groups are significantly different from each other (apart from CO₂ treatments at culture day 2), the differences in gene expression patterns between the two CO₂ treatments (SIMPER analysis) are relatively small (Table 5), ranging from 2.60% difference at culture day 2 (not significant) over 3.06% at culture day 7 (significant) to 4.30% difference at culture day 4 (significant). At culture days 2 and 4, differences between treatment groups were mainly based on expression of SM30B and ATP-synthase, contributing with 15.3% (SM30B, day 2), 8.5% (ATP-synthase, day 2), 14.6% (SM30B, day 4) and 12.7% (ATP-synthase, day 4) to the observed patterns (Fig. 2). ATP-synthase also contributed to differences between treatments at day 7 with 14.8%, with SERCA being the second most important gene at culture day 7 with a 10.6% expression level.

Taking into account that the morphological data suggest a CO₂ induced growth delay (Stumpp et al., in press) and that developmental time has a much larger effect on gene expression patterns than seawater pCO₂, it becomes immediately evident that any significant differences between CO₂ treatments could reflect normal patterns of expression expected at an earlier larval stage, thus a developmental delay “artifact” rather than a “true” CO₂ effect. Here, we compare expression patterns by plotting expression against body length (Fig. 4, and suppl. materials). On the one hand, significant differences between CO₂ treatments can become more obvious when correcting for larval growth as e.g. in the case of ATP-synthase (Fig. 4A) or non significant changes may become significant, as e.g. in CA15 (Fig. 4G). On the other hand, changes in expression that appeared significant by comparing them at culture time points, appear to be developmental effects, e.g. as in CA10 (Fig. 4H at day 2). However, the differences in transcript levels of genes that contributed most to the principal components 1 and 2 (e.g. msp130, SM30B, SM50, ATP-synthase and Na⁺/K⁺-ATPase) were even enhanced by the (visual) analysis of expression vs. body length (Fig. 4).

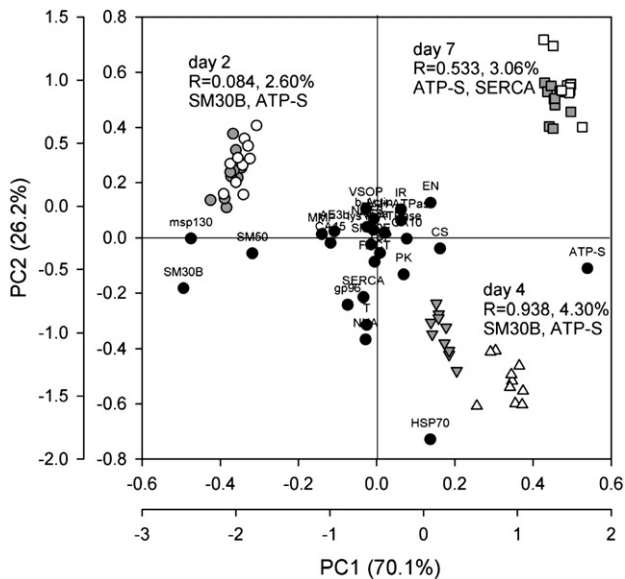


Fig. 3. Principal component analysis of gene expression patterns in control (pH 8.1, grey symbols) and high pCO₂ treated (pH 7.7, white symbols) *S. purpuratus* larvae at different time points post-fertilization (day 2 circles; day 4 triangles; day 7 squares). Sample plot for the principal components PC1 and PC2 (outer axes) and superimposed loading plot (inner axes) with the relevant genes (black circles). The plot also includes R values (one-way ANOSIM based on Bray-Curtis dissimilarity matrix) for differences (%), SIMPER results) in gene patterns between CO₂ treatments within each culture age group and the two genes that contribute most to these differences (SIMPER results).

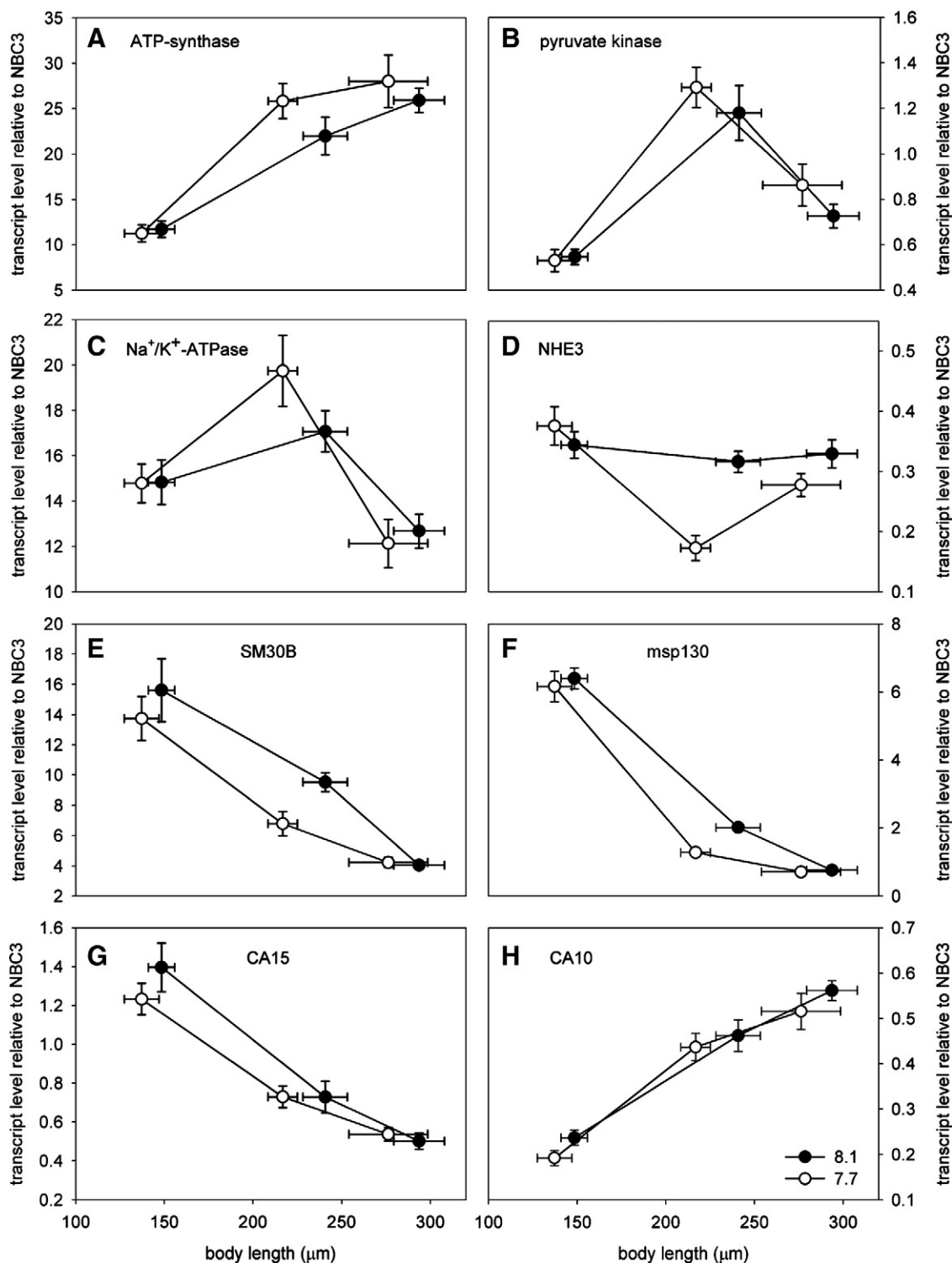


Fig. 4. Transcript levels relative to NBC3 during larval growth (body length in μm) in *S. purpuratus* larvae. A, B: metabolism: ATP-synthase, pyruvate kinase transcript levels C, D: ion regulation: Na^+/K^+ -ATPase and NHE3 transcript levels. E–H: calcification: SM30B, msp130, CA15 and CA10 transcript levels.

4. Discussion

This study reveals the impacts of CO_2 -induced seawater acidification on gene expression in *S. purpuratus* larvae during the first week of development until the feeding pluteus larval stage. All recent studies examining gene expression pattern changes during larval development were conducted on pre-feeding or unfed larval stages (Todgham and Hofmann, 2009; O'Donnell et al., 2010). The biggest

impact of $p\text{CO}_2$ on physiological processes such as metabolism was observed in sea urchin larvae once feeding had started (Stumpp et al., in press). This study aimed at revealing changes in gene expression patterns between pre-feeding (day 2) and feeding (days 4 and 7) larval stages. The growth delay induced by elevated $p\text{CO}_2$ in *S. purpuratus* larvae was observed in a parallel study (Stumpp et al., in press). The differential regulation of genes important in calcification, metabolism and ion regulation is in accordance with results from

several other recent studies (Kurihara and Shirayama, 2004; Kurihara, 2008; Clark et al., 2009; Todgham and Hofmann, 2009; Brennand et al., 2010; O'Donnell et al., 2010).

We show that in feeding pluteus larvae, a significant up-regulation of metabolic genes can be observed in response to elevated seawater $p\text{CO}_2$. These observations correlate with strongly elevated metabolic rates (ca. 2-fold) of feeding larvae from acidified treatments (Stumpp et al., in press), which might be related to an increased energy demand for cellular homeostasis and calcification.

4.1. Mortality and growth

A slightly increased survival in response to simulated ocean acidification was observed in *S. purpuratus* larvae during the experimental period. This is in accordance with results from studies on other echinoid species, in which no increased mortality was detected (*Tripneustes gratilla*, *Pseudechinus huttoni*, *Evechinus chloroticus*, *Sterechinus neumayeri*, *Echinus mathaei*, *Hemicentrotus erythrogramma*, and *Hemicentrotus pulcherrimus*) when exposed to similar levels of acidification until the four-arm pluteus stage was reached (Kurihara and Shirayama, 2004; Kurihara, 2008; Clark et al., 2009). There are no indications of increased larval mortality during sea urchin development up to the 4-arm pluteus stage in response to levels of surface ocean acidification that can be expected within the 21st century – at least with respect to average surface ocean scenarios (Caldeira and Wickett, 2003; Caldeira and Wickett, 2005). Nevertheless, CO_2 driven acidification reduced the growth rate of *S. purpuratus* larvae during the first 7 days of development. Several other studies also reported reduced larval growth in sea urchin species (*T. gratilla*, *E. chloroticus*, *S. neumayeri*, *E. mathaei*, *H. erythrogramma*, *H. pulcherrimus*, *Lytechinus pictus*, and *P. lividus*) under moderately acidified conditions (Kurihara and Shirayama, 2004; Kurihara, 2008; Clark et al., 2009; Brennand et al., 2010; O'Donnell et al., 2010; Martin et al., 2011). In our study, larvae from the acidified treatment were not only shorter, but were also characterized by the same morphological proportions (body rod, posterolateral rod and postoral rod length proportional to the body length) as control larvae at an earlier time point post fertilization (see Stumpp et al., in press for more details).

4.2. Gene expression patterns: time vs. $p\text{CO}_2$

With increase in developmental time, expression levels of most genes changed strongly. Based on gene expression profiles of larvae, we can distinguish between different culture times using ANOSIM and PCA. The gene products most important for generation of distinct differences between groups were ATP-synthase, SM30B and Na^+/K^+ -ATPase. Na^+/K^+ -ATPase, SM30B and ATP-synthase were also the most abundant transcripts among the group of 26 assessed gene products, confirming the importance of these genes in the respective functional pathways for ion regulation, calcification and metabolism.

During the first week of development, the morphology of sea urchin larvae constantly changes. Major events are the formation of the gut, including the anus (day 2). Larval arms are formed and elongated to support feeding and motility (Smith et al., 2008). Considering these changes in larval morphology, it is not surprising that the comparison of gene expression patterns during development resulted in highly distinguishable age groups. Changes in gene expression patterns in response to high $p\text{CO}_2$ were shown to be much less pronounced. As morphological differences indicated by the difference in body length, which were greatest at culture day 4 and smallest at culture day 2, correlate with the results of the ANOSIM (e.g. highest differences in gene expression on day 4 as well), the possibility exists that these changes in gene expression may be primarily due to developmental delay (Stumpp et al., in press) rather than a direct effect of high seawater $p\text{CO}_2$ on gene expression. Similar

conclusions have also been reached in a study of gill ion transport molecule gene expression in embryonic cephalopods (Hu et al., 2011).

4.3. Seawater acidification effects on gene expression patterns

Although gene expression patterns differed more strongly in response to culture time than to CO_2 -treatment, ANOSIM demonstrated distinct changes in gene expression patterns in response to CO_2 -treatment at culture days 4 and 7, while no differences in expression patterns were found at culture day 2. This is in accordance with larval growth data, where the strongest difference in growth was observed at day 4, and a less strong effect was found at day 7. A SIMPER analysis following the ANOSIM revealed that SM30B and ATP-synthase were contributing most to the differences in gene expression pattern between control and acidified treatment at culture day 4, while ATP-synthase and SERCA were the genes contributing most to the differences in patterns at culture day 7. ATP-synthase seems to be an important gene in the responses to hypercapnia and our results are in accordance with data from Todgham and Hofmann (2009) who also found up-regulation of this gene at a moderate $p\text{CO}_2$ of 101 Pa (997 μatm) in a microarray study at 40 h post-fertilization. Furthermore, Todgham and Hofmann (2009) described down regulation of more than 80 genes of major functional pathways, including calcification, metabolism, ion regulation and the cellular stress response when they exposed early prism stage larvae (40 h post-fertilization) to $p\text{CO}_2$ values of ca. 55 Pa (543 μatm). At higher seawater $p\text{CO}_2$ (ca. 101 Pa, 997 μatm), they still observed the majority of effected genes to be down regulated (160 of 178 differentially expressed genes). However, 18 genes, including ATP-synthase, were significantly up regulated under these conditions. These findings are in accordance with our results. A further increase in CO_2 stress (142 Pa) in our older, feeding larvae resulted in a higher proportion of up-regulated metabolic genes (i.e. up-regulation of four out of five metabolic genes), while calcification-related genes were down regulated in older larvae (culture day 4) in our study as well.

4.3.1. Skeletogenesis

Calcification in sea urchin larvae is carried out by primary mesenchyme cells (PMCs). PMCs ingress into the blastocoel during gastrulation, form a syncytium and deposit calcium carbonate to construct the larval spicules within the enclosed syncytial cavity (Okazaki, 1975; Etnensohn and Malinda, 1993; Wilt, 1999; Killian and Wilt, 2008). These spicules contain both a mineral and an organic phase. Among the about 45 discovered spicule matrix proteins expressed by PMCs, SM30E and SM50 are the most abundant water soluble proteins (Mann et al., 2008). The highest contribution to the gene pattern differences between the high $p\text{CO}_2$ and the control treatment was due to SM30B expression (SIMPER results). SM30B encodes a matrix protein occurring in concentric layers within the spicule (Wilt, 2002, 2005; Killian and Wilt, 2008; Mann et al., 2008). This gene, along with other genes encoding proteins for larval spicule biomineralization, such as SM50, msp130 and a metalloproteinase, were down regulated by up to 36% (msp 130) at culture day 4. When normalizing the expression data to body length (Fig. 4E–F and Fig. S1E–H), it is obvious, that this effect is not a developmental artifact, but a primary effect of seawater acidification. The down regulation of msp130 is in accordance with Todgham and Hofmann (2009), who also observed a down regulation of this and other genes that code for Ca^{2+} binding proteins at $p\text{CO}_2$ of 101 Pa (997 μatm) 40 h post-fertilization. These authors also observed a down regulation of other calcification related genes (cyclophilins, collagens, and several carbonic anhydrases) that were not investigated in this study. In contrast to these results, CO_2 induced seawater acidification down to a pH of 7.5 ($p\text{CO}_2$ of 202 Pa, 2000 μatm) and 7.25 (365 Pa, 3600 μatm) caused a compensatory increase in transcript levels of a range of

calcification genes (*msp130*, *SM30*) in 3 day old *P. lividus* larvae (Martin et al., 2011).

Carbonic anhydrases (CAs) catalyze the reversible hydration of CO_2 to bicarbonate and protons and play important roles in biomineralization as well as in cellular pH regulation. The most highly expressed CA in *S. purpuratus* PMCs is the CA SPU_012518 (CA15, Livingston et al., 2006). Love et al. (2007) found that CA15 is dominantly expressed in PMC cells at the growing spicule tip in *Helicidaris tuberculata* and *H. erythrogramma*, implying a function in biomineralization. There was, however, no significant effect of ocean acidification on the expression of CA15. However, when correcting for the growth delay, a trend towards down regulation of CA15 expression under elevated CO_2 conditions became apparent. This correlates with the down regulation of other calcification related genes in this study. In contrast to CA15, the gene coding for a carbonic anhydrase related protein (CA10) studied here does not show any impact of OA when normalized to body length. Todgham and Hofmann (2009) found an up regulation of CA15 (SPU_012518) under high seawater $p\text{CO}_2$ at 40 h post-fertilization.

The often observed growth delay in sea urchin larvae raised under high CO_2 conditions (Kurihara and Shirayama, 2004; Kurihara, 2008; Clark et al., 2009; Brennand et al., 2010; O'Donnell et al., 2010), could so far not be causally related to reduced calcification. It was even shown, that calcification rates were not altered independently of somatic growth in response to elevated seawater $p\text{CO}_2$ (Martin et al., 2011). When investigating the microstructure of larval spicules, Clark et al. (2009) noted eroded surface structures in two out of four sea urchin species at a $p\text{CO}_2$ of ca. 130 Pa (pH 7.7). Considering the down regulation of matrix protein genes observed in this and other studies (Todgham and Hofmann, 2009; O'Donnell et al., 2010) and their assumed role in the stabilization of the transient ACC phase that is precipitated in intracellular compartments (Raz et al., 2003; Killian and Wilt, 2008), it is possible that disturbances in the balance between the coordinated production of mineral and organic matrix could affect the composition and mechanical properties of the skeleton.

The similar behavior of the impacted calcification genes in this study represented by the principal component analysis and the observed down regulation of transcription factors responsible for induction of calcification processes (Todgham and Hofmann, 2009; O'Donnell et al., 2010) indicates that possibly the entire biomineralization machinery is influenced by an upstream located transcription factor in *S. purpuratus* and *Strongylocentrotus franciscanus* larvae.

4.3.2. Ion regulation

Calcification and ion- and acid–base regulation are intrinsically linked via the creation of microenvironments for biomineralization using a specific set of ion regulatory proteins. Thus, proteins that transport Ca^{2+} , HCO_3^- and H^+ — besides the Na^+/K^+ -ATPase employed as the driving force for many secondary active transporters — are of special interest in this matter. We investigated transcription of eight ion regulation genes (two AE3 transcripts, lysosomal H^+ -ATPase, vacuolar H^+ -ATPase, NHE3, VSOP, SERCA and Na^+/K^+ -ATPase).

The majority of ion transport genes tested in this study were either not regulated or down regulated with the exception of an up regulation of NHE3 at culture day 2, Na^+/K^+ -ATPase and SERCA at culture day 4 and VSOP at culture day 7. Apart from down regulation of V-type H^+ -ATPase at culture day 7 and up regulation of NHE3 at culture day 2, both of which could be developmental artifacts (S3, supplementary material), the observed growth delays did not appear to impact the regulation of the other ion regulatory proteins significantly. Todgham and Hofmann (2009) found a down regulation of ion transport genes especially Na^+ -dependent transporters and primary active transporters such as H^+ -ATPases and Na^+/K^+ -ATPase. In contrast to the data of Todgham and Hofmann (2009), we show that Na^+/K^+ -ATPase and SERCA were up-regulated at culture day 4.

An up regulation of Na^+/K^+ -ATPase transcripts is also in accordance with the results of Martin et al. (2011).

Na^+/K^+ -ATPase activity has been proposed to require up to 77% of larval metabolism (Leong and Manahan, 1997). As an important protein also linked closely to metabolism, an up regulation of transcript levels of Na^+/K^+ -ATPase is in accordance with up regulation of metabolic gene transcription in this study. Leong and Manahan (1997) found that about half of the total Na^+/K^+ -ATPase activity is held in reserve in *S. purpuratus* larvae, but can rapidly be activated in times of higher regulatory demand, e.g. for amino acid uptake from surrounding seawater or for supporting increased cellular ion regulatory demand under acidified conditions. Apart from Na^+/K^+ -ATPase and SERCA, none of the other analyzed ion regulatory genes contributed strongly to the observed differences in gene expression patterns between the two treatment groups (SIMPER analysis).

However, a slight up regulation was observed in a voltage gated proton channel (VSOP, 16%) at day 7. Voltage gated proton channels mainly function as cost effective acid extrusion mechanisms to prevent cytosolic acidification (DeCoursey, 2008).

In contrast to Todgham and Hofmann (2009), who did not observe changes in NHE or chloride/bicarbonate exchanger (AE) transcription levels in acidified conditions, our study shows a down regulation of members from these transporter families (NHE3, SLC9A3 and AE3b, SLC4A3). However, an increased requirement for ion regulatory processes is not reflected in transcription levels of AE3b and NHE3. NHE3 is highly down regulated (45%) at culture day 4, a finding that could potentially support the “energy-turnover” model of Pörtner and coworkers (Reipschläger and Pörtner, 1996) which proposes that extracellular acidification leads to a depression of NHE due to activation of energetically more favorable transporters.

4.3.3. Metabolism

To observe whether or not ATP generating processes are impacted by increased $p\text{CO}_2$ we analyzed five genes involved in energy metabolism (e.g. ATP-synthase, CS, PK, thiolase and insulin receptor). All of them were up regulated at either culture day 4 (ATP-synthase, CS, PK, and thiolase) or day 7 (insulin receptor) with ATP-synthase majorly contributing to the observed differences in gene expression patterns between treatment groups (SIMPER analysis). A growth delay dependent effect could be excluded (S3, supplementary materials). Up regulation of metabolism related genes corresponds with the observation of elevated metabolic rates in our companion study (Stumpp et al., in press). While sea urchin larval metabolic rates increased, it was found that growth rate decreased under acidified conditions (Stumpp et al., in press). It seems that although metabolic rates are increasing to meet higher energetic demands, energy allocation to somatic growth is reduced in favor of other processes, possibly ion homeostasis and calcification or maintenance of skeletal integrity. It was shown in perfused teleost fish gills that, at unaltered metabolic rates (control vs. CO_2 exposure), energy budgets are shifted towards ion regulation and protein synthesis in high CO_2 treatments (Deigweiher et al., 2010). In sea urchin larvae of the temperate species *L. pictus*, the cost of protein synthesis remains more or less the same regardless of physiological state, e.g. developmental stage or in fed vs. non-fed larvae, and was shown to account for up to 75% of metabolic rate in feeding larvae (Pace and Manahan, 2006). Despite such a high protein synthesis rate, the deposition of protein (e.g. growth) accounted for only 21% of protein synthesis rate in 15 day pluteus larvae. Thus, protein degradation remained very high. Taking into account the high metabolic costs for ion regulation as indicated by Na^+/K^+ -ATPase activity consuming up to 77% of metabolic rate in *S. purpuratus* larvae (Leong and Manahan, 1997), most of the energy gained from aerobic metabolism is used for the maintenance, e.g. cellular ion homeostasis and protein turnover, with comparatively little protein deposition, e.g. growth. A CO_2 induced increase in metabolic rate with equal feeding rate will therefore likely lead to a

growth delay. In most organisms such as fish, crustaceans, molluscs, as well as plants, it has been shown that environmental stress usually leads to a growth delay in favor of adaptive or defense mechanisms (Sumpter, 1992; Van Weerd and Komen, 1998; Matyssek et al., 2002; Verslycke and Janssen, 2002; Verslycke et al., 2004; Voronezhskaya et al., 2004). The (potential) hypercapnia induced reallocation of energy towards vital processes such as ion homeostasis and calcification remains to be studied in future projects.

5. Conclusion

We have investigated how gene expression patterns change in response to simulated ocean acidification in pre-feeding and feeding *S. purpuratus* larvae. We showed that gene expression patterns strongly correlate with developmental stage and growth. This could lead to a misinterpretation of results should gene expression analyses be simply normalized on a temporal scale. For an adequate evaluation of gene expression patterns as well as other physiological processes during embryonic and larval development, we conclude that it is essential to closely monitor larval morphology and increase the sampling frequency in order to be able to distinguish between effects of elevated $p\text{CO}_2$ and effects related to delayed, but otherwise normal, developmental programs. Despite the potential growth delay related effects on gene expression pattern, we found genes that were differentially regulated under acidification stress. Metabolic genes were up-regulated in order to meet the higher energetic demands, while key calcification genes were down-regulated. Nevertheless, to support and understand the present gene expression data, mechanistic studies on energy budgets, extra- and intracellular pH homeostasis and calcification in sea urchin larvae are urgently needed.

Acknowledgements

MS and FM are funded by the DFG Excellence cluster 'Future Ocean' and the German 'Biological impacts of ocean acidification (BIOACID)' project 3.1.4, funded by the Federal Ministry of Education and Research (BMBF, FKZ 03F0608A). SD is funded by the Linnaeus Centre for Marine Evolutionary Biology at the University of Gothenburg (<http://www.cemeb.science.gu.se/>), and supported by a Linnaeus-grant from the Swedish Research Councils VR and Formas; VR and Formas grants to MT; Knut and Alice Wallenberg's minnen and the Royal Swedish Academy of Sciences.

The authors thank T. Reusch for use of his qRT-PCR machine and we are grateful to N. Bergmann and U. Panknin for valuable advice (NB) and help with carrying out the qRT-PCR (UP).

References

Andersen, C.L., Jensen, J.L., Ormtoft, T.F., 2004. Normalization of real-time quantitative reverse transcription-PCR data: a model-based variance estimation approach to identify genes suited for normalization, applied to bladder and colon cancer data sets. *Cancer Res.* 64, 5245–5250.

Brennand, H.S., Soars, N., Dworjanyn, S.A., Davis, A.R., Byrne, M., 2010. Impact of ocean warming and ocean acidification on larval development and calcification in the sea urchin *Triplonastes gratilla*. *Plos One* 5, e11372.

Byrne, M., Ho, M., Selvakumaraswamy, P., Nguyen, H.D., Dworjanyn, S.A., Davis, A.R., 2009. Temperature, but not pH, compromises sea urchin fertilization and early development under near-future climate change scenarios. *Proc. R. Soc. B Biol.* 276, 1883–1888.

Byrne, M., Soars, N., Ho, M., Wong, E., McElroy, D., Selvakumaraswamy, P., Dworjanyn, S.A., Davis, A.R., 2010b. Fertilization in a suite of coastal marine invertebrates from south east Australia is robust to near-future ocean warming and acidification. *Mar. Biol.* 157, 2061–2069.

Byrne, M., Soars, N., Selvakumaraswamy, P., Dworjanyn, S.A., Davis, A.R., 2010a. Sea urchin fertilization in a warm, acidified and high $p\text{CO}_2$ ocean across a range of sperm densities. *Mar. Environ. Res.* 69, 234–239.

Caldeira, K., Wickert, M.E., 2003. Anthropogenic carbon and ocean pH. *Nature* 425, 365.

Caldeira, K., Wickert, M.E., 2005. Ocean model predictions of chemistry changes from carbon dioxide emissions to the atmosphere and ocean. *J. Geophys. Res.* 110.

Cao, L., Caldeira, K., 2008. Atmospheric CO_2 stabilization and ocean acidification. *Geophys. Res. Lett.* 35.

Carr, R.S., Biedenbach, J.M., Nipper, M., 2006. Influence of potentially confounding factors on sea urchin porewater toxicity tests. *Arch. Environ. Contam. Toxicol.* 51, 573–579.

Clark, D., Lamare, M., Barker, M., 2009. Response of sea urchin pluteus larvae (Echinodermata: Echinoidea) to reduced seawater pH: a comparison among tropical, temperate, and a polar species. *Mar. Biol.* 156, 1125–1137.

DeCoursey, T.E., 2008. Voltage-gated proton channels. *Cell Mol. Life Sci.* 65, 2554–2573.

Deigweier, K., Hirse, T., Bock, C., Lucassen, M., Pörtner, H.-O., 2010. Hypercapnia induced shifts in gill energy budgets of Antarctic notothenioids. *J. Comp. Physiol. B* 180, 347–359.

Dupont, S., Havenhand, J., Thorndyke, W., Peck, L., Thorndyke, M.C., 2008. CO_2 -driven ocean acidification radically affect larval survival and development in the brittlestar *Ophiotrix fragilis*. *Mar. Ecol. Prog. Ser.* 373, 285–294.

Dupont, S., Lundve, B., Thorndyke, M., 2010a. Near future ocean acidification increases growth rate of the lecithotrophic larvae and juveniles of the sea star *Crossaster papposus*. *J. Exp. Zool. B* 314B, 382–389.

Dupont, S., Ortega-Martinez, O., Thorndyke, M.C., 2010b. Impact of near-future ocean acidification on echinoderms. *Ecotoxicology* 19, 449–462.

Ericson, J.A., Lamare, M.D., Morley, S.A., Barker, M.F., 2010. The response of two ecologically important Antarctic invertebrates (*Sterechinus neumayeri* and *Parborlasia corrugatus*) to reduced seawater pH: effects on fertilisation and embryonic development. *Mar. Biol.* 157, 2689–2702.

Ettensohn, C.A., Malinda, K.M., 1993. Size regulation and morphogenesis: a cellular analysis of skeletogenesis in the sea urchin embryo. *Development* 119, 155–167.

Fabry, V.J., 2008. Marine calcifiers in a high- CO_2 ocean. *Science* 320, 1020–1022.

Guillard, R.R.L., Ryther, J.H., 1962. Studies of marine planktonic diatoms. I. *Cyclotella nana* (Husted), and *Detonula confervacea* (Cleve). *Can. J. Microbiol.* 8, 229–239.

Gutowska, M.A., Melzner, F., Pörtner, H.-O., Meier, S., 2010. Calcification in the cephalopod *Sepia officinalis* in response to elevated seawater $p\text{CO}_2$. *Mar. Biol.* 157, 1653–1663.

Gutowska, M.A., Pörtner, H.-O., Melzner, F., 2008. Growth and calcification in the cephalopod *Sepia officinalis* under elevated seawater $p\text{CO}_2$. *Mar. Ecol. Prog. Ser.* 373, 303–309.

Havenhand, J., Buttler, F.R., Thorndyke, M.C., Williamson, J.E., 2008. Near-future levels of ocean acidification reduce fertilization success in a sea urchin. *Curr. Biol.* 18, R651–R652.

Hoegh-Guldberg, O., Mumby, P.J., Hooten, A.J., Steneck, R.S., Greenfield, P., Gomez, E., Harvell, C.D., Sale, P.F., Edwards, A.J., Caldeira, K., Knowlton, N., Eakin, C.M., Iglesias-Prieto, R., Muthiga, N., Bradbury, R.H., Dubi, A., Hatziolos, M.E., 2007. Coral reefs under rapid climate change and ocean acidification. *Science* 318, 1737–1742.

Hu, M.Y.-A., Tseng, Y.-C., Stumpp, M., Gutowska, M.A., Kiko, R., Lucassen, M., Melzner, F., 2011. Elevated seawater $p\text{CO}_2$ differentially affects branchial acid–base transporters over the course of development in the cephalopod *Sepia officinalis*. *Am. J. Physiol.* 300, R1100–R1114.

Killian, C.E., Wilt, F.H., 2008. Molecular aspects of biomineralization of the echinoderm endoskeleton. *Chem. Rev.* 106, 4463–4474.

Kurihara, H., 2008. Effects of CO_2 -driven ocean acidification on the early developmental stages of invertebrates. *Mar. Ecol. Prog. Ser.* 373, 275–284.

Kurihara, H., Shirayama, Y., 2004. Effects of increased atmospheric CO_2 on sea urchin early development. *Mar. Ecol. Prog. Ser.* 274, 161–169.

Langdon, C., Atkinson, M.J., 2005. Effect of elevated $p\text{CO}_2$ on photosynthesis and calcification of corals and interactions with seasonal change in temperature/irradiance and nutrient enrichment. *J. Geophys. Res.* 110.

Leong, P.K.K., Manahan, D.T., 1997. Metabolic importance of Na^+/K^+ -ATPase activity during sea urchin development. *J. Exp. Biol.* 200, 2881–2892.

Lewis, E., Wallace, D.W.R., 1998. CO2SYS—program developed for the CO_2 system calculations. Carbon Dioxide Inf Anal Center Report ORNL/CDIAC-105.

Livak, K.J., Schmittgen, T.D., 2001. Analysis of relative gene expression data using real-time quantitative PCR and the $2^{-\Delta\Delta\text{CT}}$ method. *Methods* 25, 402–408.

Livingston, B.T., Killian, C., Wilt, F., Cameron, A., Landrum, M.J., Ermolaeva, O., Sapojnikov, V., Maglott, D.R., Buchanan, A.M., Ettensohn, C.A., 2006. A genome-wide analysis of biomineralization-related proteins in the sea urchin *Strongylocentrotus purpuratus*. *Dev. Biol.* 300, 335–348.

Love, A.C., Andrews, M.E., Raff, R.A., 2007. Gene expression patterns in a novel animal appendage: the sea urchin pluteus arm. *Evol. Dev.* 9, 51–68.

Mann, K., Poustka, A.J., Mann, M., 2008. The sea urchin (*Strongylocentrotus purpuratus*) test and spine proteomes. *Proteome Sci.* 6, 33.

Martin, S., Richier, S., Pedrotti, M.-L., Dupont, S., Castejon, C., Gerakis, Y., Kerros, M.-E., Oberhänsli, F., Teyssié, J.-L., Gattuso, J.P., 2011. Early development and molecular plasticity in the Mediterranean sea urchin *Paracentrotus lividus* exposed to CO_2 driven ocean acidification. *J. Exp. Biol.* 214, 1357–1368.

Matyssek, R., Schnyder, H., Elstner, E.F., Munch, J.C., Pretzsch, H., Sandermann, H., 2002. Growth and parasite defence in plants: the balance between resource sequestration and retention: in lieu of a guest editorial. *Plant Biol.* 4, 133–136.

Melzner, F., Gutowska, M.A., Langenbuch, M., Dupont, S., Lucassen, M., Thorndyke, M.C., Bleich, M., Pörtner, H.-O., 2009. Physiological basis for high CO_2 tolerance in marine ectothermic animals: pre-adaptation through lifestyle and ontogeny? *Biogeosciences* 6, 2313–2331.

O'Donnell, M.J., Todgham, A.E., Sewell, M.A., Hammond, L.M., Ruggiero, K., Fangue, N.A., Zippay, M.L., Hofmann, G.E., 2010. Ocean acidification alters skeletogenesis and gene expression in larval sea urchins. *Mar. Ecol. Prog. Ser.* 398, 157–171.

Okazaki, K., 1975. Spicule formation by isolated micromeres of the sea urchin embryo. *Am. Zool.* 15, 567–581.

Orr, J.C., Fabry, V.J., Aumont, O., Bopp, L., Doney, S.C., Feely, R.A., Gnanadesikan, A., Gruber, N., Ishida, A., Joos, F., Key, R.M., Lindsay, K., Maier-Reimer, E., Matar, R., Mofray, P., Mouchet, A., Najjar, R.G., Plattner, G.-K., Rodgers, K.B., Sabine, C.L.,

- Sarmiento, J.L., Schlitzer, R., Slater, R.D., Totterdell, I.J., Weirig, M.-F., Yamanaka, Y., Yool, A., 2005. Anthropogenic ocean acidification over the twenty-first century and its impact on calcifying organisms. *Nature* 437, 681–686.
- Pace, D.A., Manahan, D.T., 2006. Fixed metabolic costs for highly variable rates of protein synthesis in sea urchin embryos and larvae. *J. Exp. Biol.* 209, 391–392.
- Pörtner, H.-O., 2008. Ecosystem effects of ocean acidification in times of ocean warming: a physiologist's view. *Mar. Ecol. Prog. Ser.* 373, 203–217.
- Pörtner, H.-O., Farrell, A.P., 2008. Physiology and climate change. *Science* 322, 90–92.
- Ramakers, C., Ruijter, J.M., Deprez, R.H., Moorman, A.F., 2003. Assumption-free analysis of quantitative real-time polymerase chain reaction (PCR) data. *Neurosci. Lett.* 13, 62–66.
- Raz, S., Hamilton, P.C., Wilt, F.H., Weiner, S., Addadi, L., 2003. The transient phase of amorphous calcium carbonate in sea urchin larval spicules: the involvement of proteins and magnesium ions in its formation and stabilization. *Adv. Funct. Mater.* 13, 480–486.
- Reipschläger, A., Pörtner, H.-O., 1996. Metabolic depression during environmental stress: the role of extracellular versus intracellular pH in *Sipunculus nudus*. *J. Exp. Biol.* 199, 1801–1807.
- Sarazin, G., Michard, G., Prevot, F., 1999. A rapid and accurate spectroscopic method for alkalinity measurements in seawater samples. *Water Res.* 33, 290–294.
- Shirayama, Y., Thornton, H., 2005. Effect of increased atmospheric CO₂ on shallow water marine benthos. *J. Geophys. Res.* 110.
- Smith, M.M., Smith, L.C., Cameron, A., Urry, L.A., 2008. The larval stages of the sea urchin, *Strongylocentrotus purpuratus*. *J. Morphol.* 269, 713–733.
- Stumpp M., Wren J., Melzner F., Thorndyke M.C., Dupont S., in press. CO₂ induced seawater acidification impacts sea urchin larval development I: elevated metabolic rates decrease scope for growth and induce developmental delay. *Comp Biochem Physiol A*. doi:10.1016/j.cbpa.2011.06.022.
- Sumpter, J.P., 1992. Control of growth of rainbow trout (*Oncorhynchus mykiss*). *Aquaculture* 100, 299–320.
- Thomsen, J., Gutowska, M.A., Saphörster, J., Heinemann, A., Fietzke, J., Hiebenthal, C., Eisenhauer, A., Körtzinger, A., Wahl, M., Melzner, F., 2010. Calcifying invertebrates succeed in a naturally CO₂ enriched coastal habitat but are threatened by high levels of future acidification. *Biogeosciences* 7, 3879–3891.
- Thomsen, J., Melzner, F., 2010. Seawater acidification does not elicit metabolic depression in the blue mussel *Mytilus edulis*. *Mar. Biol.* 157, 2667–2676.
- Todgham, A.E., Hofmann, G.E., 2009. Transcriptomic response of sea urchin larvae *Strongylocentrotus purpuratus* to CO₂-driven seawater acidification. *J. Exp. Biol.* 212, 2579–2594.
- Van Weerd, J.H., Komen, J., 1998. The effects of chronic stress on growth in fish: a critical appraisal. *Comp. Biochem. Physiol. A* 120, 107–112.
- Vandenbroucke, I.I., Vandesompele, J., De Paep, A., Messiaen, L., 2001. Quantification of splice variants using real-time PCR. *Nucleic Acids Res.* 29, e68.
- Verslycke, T., Janssen, C.R., 2002. Effects of a changing abiotic environment on the energy metabolism in the estuarine mysid shrimp *Neomysis integer* (Crustacea: Mysidacea). *J. Exp. Mar. Biol. Ecol.* 279, 61–72.
- Verslycke, T., Roast, S.D., Widdows, J., Jones, M.B., Janssen, C.R., 2004. Cellular energy allocation and scope for growth in the estuarine mysid *Neomysis integer* (Crustacea: Mysidacea) following chlorpyrifos exposure: a method comparison. *J. Exp. Mar. Biol. Ecol.* 306, 1–16.
- Voronezhskaya, E.E., Khabarova, M.Y., Nezlin, L.P., 2004. Apical sensory neurones mediate developmental retardation induced by conspecific environmental stimuli in freshwater pulmonate snails. *Development* 131, 3671–3680.
- Wilt, F.H., 1999. Matrix and mineral in the sea urchin larval skeleton. *J. Struct. Biol.* 126, 216–226.
- Wilt, F.H., 2002. Biomineralization of the spicules of sea urchin embryos. *Zool Sci.* 19, 253–261.
- Wilt, F.H., 2005. Developmental biology meets materials science: morphogenesis of biomineralized structures. *Dev. Biol.* 280, 15–25.
- Wood, H.L., Spicer, J.I., Widdicombe, S., 2008. Ocean acidification may increase calcification rates, but at a cost. *Proc. R. Soc. B Biol.* 275, 1767–1773.